



HAL
open science

Surface recombination in doped semiconductors: Effect of light excitation power and of surface passivation

Fabian Cadiz, D. Paget, A. Rowe, V. Berkovits, V. Ulin, S. Arscott, Emilien Peytavit

► **To cite this version:**

Fabian Cadiz, D. Paget, A. Rowe, V. Berkovits, V. Ulin, et al.. Surface recombination in doped semiconductors: Effect of light excitation power and of surface passivation. *Journal of Applied Physics*, 2013, 114 (10), pp.103711. <10.1063/1.4821139>. <hal-02345653>

HAL Id: hal-02345653

<https://hal.science/hal-02345653v1>

Submitted on 25 May 2022

HAL is a multi-disciplinary open access archive for the deposit and dissemination of scientific research documents, whether they are published or not. The documents may come from teaching and research institutions in France or abroad, or from public or private research centers.

L'archive ouverte pluridisciplinaire **HAL**, est destinée au dépôt et à la diffusion de documents scientifiques de niveau recherche, publiés ou non, émanant des établissements d'enseignement et de recherche français ou étrangers, des laboratoires publics ou privés.



HAL Authorization

Surface recombination in doped semiconductors: Effect of light excitation power and of surface passivation

Cite as: J. Appl. Phys. **114**, 103711 (2013); <https://doi.org/10.1063/1.4821139>

Submitted: 15 May 2013 • Accepted: 28 August 2013 • Published Online: 13 September 2013

F. Cadiz, D. Paget, A. C. H. Rowe, et al.



View Online



Export Citation



CrossMark

ARTICLES YOU MAY BE INTERESTED IN

[On effective surface recombination parameters](#)

Journal of Applied Physics **116**, 014503 (2014); <https://doi.org/10.1063/1.4886595>

[Determination of effective surface recombination velocity and minority-carrier lifetime in high-efficiency Si solar cells](#)

Journal of Applied Physics **54**, 238 (1983); <https://doi.org/10.1063/1.331693>

[Detailed Balance Limit of Efficiency of p-n Junction Solar Cells](#)

Journal of Applied Physics **32**, 510 (1961); <https://doi.org/10.1063/1.1736034>

Lock-in Amplifiers
up to 600 MHz



Zurich
Instruments



Surface recombination in doped semiconductors: Effect of light excitation power and of surface passivation

F. Cadiz,¹ D. Paget,^{1,a)} A. C. H. Rowe,¹ V. L. Berkovits,² V. P. Ulin,² S. Arscott,³ and E. Peytavit³

¹*Physique de la matière condensée, Ecole Polytechnique, CNRS, 91128 Palaiseau, France*

²*A. F. Ioffe Physico-technical Institute, 194021 Saint Petersburg, Russia*

³*Institut d'Electronique, de Microélectronique et de Nanotechnologie (IEMN), University of Lille, CNRS, Avenue Poincaré, Cité Scientifique, 59652 Villeneuve d'Ascq, France*

(Received 15 May 2013; accepted 28 August 2013; published online 13 September 2013)

For n- and p-type semiconductors doped above the 10^{16} cm^{-3} range, simple analytical expressions for the surface recombination velocity S have been obtained as a function of excitation power P and surface state density N_T . These predictions are in excellent agreement with measurements on p-type GaAs films, using a novel polarized microluminescence technique. The effect on S of surface passivation is a combination of the changes of three factors, each of which depends on N_T : (i) a power-independent factor which is inversely proportional to N_T and (ii) two factors which reveal the effect of photovoltage and the shift of the electron surface quasi Fermi level, respectively. In the whole range of accessible excitation powers, these two factors play a significant role so that S always depends on power. Three physical regimes are outlined. In the first regime, illustrated experimentally by the oxidized GaAs surface, S depends on P as a power law of exponent determined by N_T . A decrease of S such as the one induced by sulfide passivation is caused by a marginal decrease of N_T . In a second regime, as illustrated by GaInP-encapsulated GaAs, because of the reduced value of S , the photoelectron concentration in the subsurface depletion layer can no longer be neglected. Thus, S^{-1} depends logarithmically on P and very weakly on surface state density. In a third regime, expected at extremely small values of P , the photovoltage is comparable to the thermal energy, and S increases with P and decreases with increasing N_T . © 2013 AIP Publishing LLC. [<http://dx.doi.org/10.1063/1.4821139>]

I. INTRODUCTION

The investigation of semiconductor surface passivation has a renewed interest because of the strong development of bipolar nanoelectronics,¹ and of high surface-to-volume ratio structures such as nanowires.⁴ After the early theoretical investigations which apply to the surface the Shockley Read Hall formalism (SRH) and obtain an expression of the surface recombination velocity S ,⁵ surface recombination has been extensively explored using photoconductivity,^{6,7} surface photovoltage measurements,⁸ scanning electron microscopy,⁹ cathodoluminescence,¹⁰ or photoluminescence^{11–13} on a wide range of materials including GaAs,¹² Si,¹⁴ InP,¹⁵ GaN,¹⁶ InN,¹⁷ ZnSe,¹⁸ and alloys.¹⁹ However, the immense majority of these works rely on the usual hypothesis that S , as defined by the SRH formalism, is proportional to the surface density of states, and is a fundamental parameter for describing the surface electronic properties. To the best of our knowledge, only two works, one at the Si/SiO₂ interface¹⁴ and the other on GaAs surfaces,¹ have investigated the dependence of S on excitation power and surface density of states. From a theoretical point of view, the most comprehensive treatments of the problem rely heavily on computer simulations.^{1,14,20} In short, a simple description of the dependence of S on power and on surface density of states is still lacking.

Here, we present an experimental and theoretical investigation of surface recombination with emphasis on the power dependence of S and on the origin for its decrease induced by surface passivation. The surface recombination velocity S of p^+ GaAs films is measured using an original technique based on imaging of the luminescence under tightly focused light excitation.²¹ The experimental results are in quantitative agreement with the predictions of a model valid for p- or n-type doped semiconductors (above the 10^{16} cm^{-3} range). This model gives a simple analytical expression for S as the product of a power-independent quantity S_0 and of two factors expressing the effect on surface recombination of photovoltage and of the shift of the electron surface quasi Fermi level, respectively. Surprisingly, S_0 is inversely proportional to the surface density of states, and is thus increased by passivation. However, since the power-dependent factors also depend on surface state density, the observed passivation-induced decrease of S is a combined effect of the changes of S_0 and of the above two factors. It is concluded that the decrease of S by one order of magnitude induced by sulfide passivation is caused by a marginal decrease of N_T , and that for a GaInP-encapsulated surface, S is almost independent on N_T .

The paper is organized as follows. In Sec. II, we obtain an analytical expression for S as a function of light excitation power and surface state density. The experimental method is explained in Sec. III and the results are presented in Sec. IV and discussed in Sec. V.

^{a)}Electronic address: daniel.paget@polytechnique.edu

II. THEORY

In this section, we show that simple expressions for S can be obtained. Fig. 1 summarizes the near surface band structure scheme which will be used in the specific case of p-type material.²² When photo-excited, a steady-state photo-electron concentration is established whose value at the edge of the depletion zone is n_0 . This results in a photo-current of magnitude

$$J_p = qn_0S, \quad (1)$$

where q is the absolute value of the electron charge. Here, the photo-current generated within the depletion zone is neglected, which, for an excitation energy slightly above bandgap, is valid for doping levels larger than several 10^{16} cm^{-3} . Injection of photo-electrons creates a surface quasi equilibrium characterized by an electron quasi-Fermi level at energy qV_s above its position in the bulk, where qV_s is the photovoltage shifted by $\Delta\phi$ with respect to its position in the dark. As seen from Fig. 1, the surface barrier is given by

$$\phi_b = \phi_0 + \Delta\phi - qV_s, \quad (2)$$

where ϕ_0 is the barrier value in the dark. The Schottky current is given by

$$J_s = J_0 \exp\left[-\frac{\Delta\phi}{k_B T}\right] \left(\exp\left[\frac{qV_s}{k_B T}\right] - 1\right). \quad (3)$$

Here, the saturation current J_0 is related to the effective Richardson constant A^{**} and to the surface barrier in the dark ϕ_0 by $J_0 = A^{**} T^2 \exp[-\phi_0/k_B T]$.

The surface recombination current J_r , given by the SRH expression,⁵ is obtained by integration over centers situated between the hole and electron quasi Fermi levels since

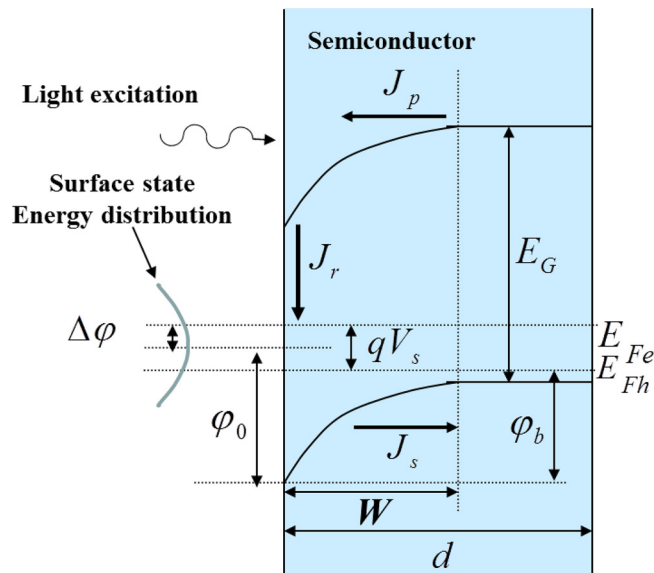


FIG. 1. A schematic representation of the band structure of the photo-excited GaAs film of thickness d showing the light-induced shift of the surface electron Fermi level, $\Delta\phi$, and the photovoltage qV_s . Also shown are the photocurrent J_p and the Schottky current J_s .

centers situated below E_{Fh} are occupied and centers situated above E_{Fe} are empty

$$J_r = q \int_{E_{Fh}}^{E_{Fe}} N_T(\epsilon) \frac{\sigma_n \nu_n \sigma_p \nu_p (n_s p_s - n_{ts} p_{ts})}{\sigma_p \nu_p (p_s + p_{ts}) + \sigma_n \nu_n (n_s + n_{ts})} d\epsilon, \quad (4)$$

where $N_T(\epsilon)$ is the surface concentration of defects per unit energy at an energy ϵ above the position of the Fermi level at equilibrium. Here, $\sigma_n(\sigma_p)$ and $\nu_n(\nu_p)$ are the electron (hole) capture cross sections at the centers and thermal velocities, respectively, $n_s(p_s)$ are the volume concentrations of electrons (holes) at the surface, and $n_{ts}(p_{ts})$ are their values at equilibrium if the Fermi level coincides with the energy (ϵ) of the surface centers. While Eq. (4) has been verified by studies on the Si/SiO₂ interface as a function of electric field,²³ this equation implies that surface recombination strongly depends on the photoelectron concentrations at the surface n_s and at the edge of the depletion region n_0 , respectively. Both n_s and n_0 are in turn dependent on the excitation power and/or on surface recombination itself so that Eq. (3) should be solved self-consistently and cannot give a fundamental expression for S .

We also assume that the centers which cause surface recombination are also those responsible for Fermi level pinning. This excludes materials such as InP.¹⁵ As shown in Appendix A, surface recombination is limited by hole capture. This implies that the occupation probability of centers between E_{Fh} and E_{Fe} is close to unity and that the centers which dominate the surface recombination are situated near the electron quasi Fermi level, in a typical energy width of $k_B T$. Their volume concentration is $N_T^*(\Delta\phi) = N_T(\Delta\phi) k_B T / a$, where a is a typical thickness of the surface layer.

The shape of the function $N_T(\epsilon)$ has been investigated both for metal-semiconductor interfaces² and for insulator-semiconductor interfaces.³ It has been found that near midgap $N_T(\epsilon)$ is relatively flat and that the energy of the minimum of $N_T(\epsilon)$ corresponds with the energy at which the Fermi level is pinned. Thus, the volume concentration of defects will be taken as

$$N_T^*(\Delta\phi) = N_T^*(0) = N_T(0) k_B T / a. \quad (5)$$

This equation is valid at relatively low excitation power if $\Delta\phi$ is not too large.

Shown in Appendix B is a calculation of S using charge and current conservation and assuming equilibrium between the surface and the bulk. The final result is that S can be expressed as the product of a quantity S_0 independent on power and of two factors, which as shown in Eq. (B2) reflect the shift $\Delta\phi$ of the Fermi level and the photovoltage, respectively.

$$S = S_0 \exp\left[-\frac{\Delta\phi}{k_B T}\right] \left\{ 1 - K \exp\left[-(1 + \eta^{-1}) \frac{\Delta\phi}{k_B T}\right] \right\}. \quad (6)$$

The quantity S_0 is given by

$$S_0 = \frac{J_0^2}{q N_T^*(0) J_{r0}} \exp\left[\frac{\phi_0}{k_B T}\right], \quad (7)$$

where the current J_{r0} is given by

$$J_{r0} = q\nu_p n_i (a n_i \sigma_p). \quad (8)$$

The number

$$\eta = \frac{\varepsilon}{qW_0 N_T(0)} \quad (9)$$

is a measure of the ratio of surface charge to the charge in the depletion zone. Here, ε is the semiconductor permittivity. The quantity K is given by

$$K = \exp \left[\frac{\Delta\phi^2}{4\eta^2 \varphi_0 k_B T} - \gamma \exp \left[\frac{\Delta\phi}{k_B T} \right] \right], \quad (10)$$

where

$$\gamma = \frac{A^{**} T^2}{qS_0 N_A}. \quad (11)$$

The quantity K is equal to unity if the photoelectron charge in the depletion layer is negligible with respect to the fixed acceptor charge (second factor of Eq. (10)) and if $\varphi_b - \varphi_0 \ll \varphi_0$ (first factor). Equation (6) is valid provided surface recombination is not limited by thermal injection of minority carriers, otherwise one has $S = v_n \approx 3 \times 10^7$ cm/s for p-type GaAs. The light-induced motion $\Delta\phi$ of the electron quasi Fermi level is given by the following equation:

$$K \xi \exp \left[\frac{\Delta\phi}{k_B T} \right] - \exp \left[\frac{\Delta\phi}{k_B T} (1 + \eta^{-1}) \right] - K = -\frac{v_d}{S_0} \exp \left[\frac{\Delta\phi}{k_B T} (2 + \eta^{-1}) \right], \quad (12)$$

where the reduced power is given by

$$\xi = qv_d N_0 / J_0. \quad (13)$$

The quantity N_0 , proportional to excitation power but independent on surface recombination, is the reduced electron concentration. Expressions for N_0 and for the diffusion velocity v_d are given by Eqs. (B8) and (B11), respectively.

Equations (6) and (12) are the fundamental equations of the present work. They allow us to calculate S for a given light excitation power and surface state density, with approximations listed in Appendix A. Note that although the calculation has been explained for a p-type material, the latter equations are equally valid for n-type provided majority and minority carriers are interchanged. The only difference is that Eq. (8) should be replaced by $J_{r0} = qv_n n_i (a n_i \sigma_n)$.

Since the right hand side of Eq. (12) is negligible because v_d , as shown below, is small with respect to S_0 , three power regimes can be identified where S has an analytical expression. At very low excitation power ($\xi \ll 1$), one has $\Delta\phi \ll k_B T$ so that $K \approx 1$. In Eq. (6), since qV_s is comparable to $k_B T$, the value of S is determined by that of S_0 and by the factor which multiplies K . To first order in $\Delta\phi/k_B T$, we obtain

$$S \approx S_0 \xi = v_d \frac{A^{**} T^2}{J_{r0}} \frac{N_0}{N_T^*(0)} \quad (14)$$

so that S increases linearly with N_0 as observed for silicon.²⁴ Another regime occurs at higher excitation power such that $\xi \gg 1$ provided K remains close to unity (i.e., if $\gamma \ll 1$) implying that the photoelectron concentration in the depletion layer is smaller than the acceptor concentration. In this case, the last term on the left hand side of Eq. (12) is negligible and one finds

$$S \approx S_0 \xi^{-\eta} \quad (15)$$

so that S decreases with N_0 as a power law of exponent $-\eta$ under the dominant effect of the second factor of Eq. (6). At even larger excitation powers, or for a reduced surface state density, a large concentration of photo-electrons accumulates at the surface and $n_s/N_A \gg \varphi_0/k_B T$ implying in Eq. (B3) that $\Delta\phi \gg k_B T$ and $K \ll 1$. Equation (12) simplifies to $K \exp[-\Delta\phi/\eta k_B T] = 1/\xi$ for which the dominant factor on the left hand side is the double exponential appearing in Eq. (10). The approximate value of S is then

$$S \approx \frac{\gamma_0 v_d}{\ln \xi}, \quad (16)$$

where γ_0 is given by

$$\gamma_0 = \frac{A^{**} T^2}{qv_d N_A}. \quad (17)$$

The quantity γ_0 is related to γ (Eq. (11)) but does not depend on S_0 so that in this regime S no longer depends on the surface state density. Upon increasing excitation power, Eq. (16) holds as long as $\Delta\phi$ is smaller than the characteristic width of the surface state distribution. For higher power, the linearized form of the charge neutrality equation [Eq. (B3)] can no longer be used, and the analytical treatment is no longer valid.

III. EXPERIMENT

A. Measurement of S

P-type ($N_A \approx 10^{17}$ cm⁻³) GaAs films of thickness $d = 3 \mu\text{m}$ are photo-excited with circularly polarized light of energy 1.59 eV. As shown in panel (a) of Fig. 2, these films are grown on a GaAs semi-insulating substrate, with a thin GaInP back interface serving as a confinement layer for the photo-electrons and ensuring $S' = 0$ at the back surface.

In order to measure S , a previously described²¹ polarized microluminescence technique illustrated in the left panel of Fig. 2 is employed. The circularly polarized light excitation is focused to a gaussian spot of half width of $0.6 \mu\text{m}$ and the resulting luminescence emission and its polarization are spectroscopically analyzed (panel (d) of Fig. 2) and imaged (see panels (b) and (c) of Fig. 2). Both σ^+ - and σ^- -polarized light excitations are in turn used to excite the sample and an image is taken of the σ^\pm polarized components of the photoluminescence with the laser being removed by an appropriate filter. The resulting four images, denoted σ^{++} , σ^{+-} , σ^{--} , and σ^{-+} , are combined to form a sum image $I_s = (\sigma^{++} + \sigma^{+-} + \sigma^{--} + \sigma^{-+})/2$ proportional to n and a difference image $I_d = (\sigma^{++} - \sigma^{+-} + \sigma^{--} - \sigma^{-+})/2$ proportional

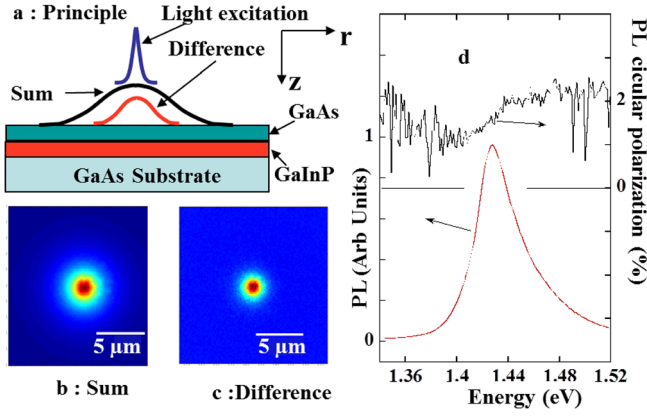


FIG. 2. Panel (a) shows the principle of the experiment. The circularly polarized laser is tightly focused on a GaAs film and the spatial distribution of the luminescence intensity and polarization are imaged. Panels (b) and (c) show typical sum and difference images, defined by Eqs. (18) and (19), for oxidized GaAs. Also shown in panel (d) are spectra of the photoluminescence and of its degree of circular polarization for the naturally oxidized surface.

to $n_+ - n_-$. Here, n_+ and n_- are the concentrations of electrons with spin aligned parallel or anti-parallel with the direction of light excitation z chosen as the direction of quantization. Typical experimental images for a naturally oxidized GaAs film are shown in panels (a) and (b) of Fig. 2, respectively. Their cross sections as a function of radial distance r to the excitation spot are given by

$$I_s(r) = A \int_0^d n(r, z) \exp[-\alpha_l z] dz \quad (18)$$

and

$$I_d(r) = A |P_i| \int_0^d (n_+ - n_-)(r, z) \exp[-\alpha_l z] dz. \quad (19)$$

Here, A is a constant and $\alpha_l \approx (3 \mu\text{m})^{-1}$ is the absorption coefficient at the luminescence energy. The quantity P_i depends on the matrix elements for recombination and is equal to ± 0.5 for σ^\mp light excitation. The quantity $n_+ - n_-$ is given by the spin diffusion equation

$$(g_+ - g_-)\tau_s \phi(r) \alpha \exp[-\alpha z] - (n_+ - n_-) + L_s^2 \Delta(n_+ - n_-) = 0, \quad (20)$$

where $(g_+ - g_-)/g = P_i$ and $L_s = \sqrt{D\tau_s}$ is the spin diffusion length. Here, τ_s , given by $\tau_s = (1/\tau + 1/T_1)^{-1}$ where T_1 is the spin-lattice relaxation time, is the spin lifetime. The boundary conditions are the same as for $n = n_+ + n_-$ in Eq. (B6).

In the case of charge transport, although the diffusion equation analogous to Eq. (B6) does not have an analytical solution, numerical calculations indicate that for $r > d$, n can be written as $n(r, z) \approx f_1(r)f_2(z)$, where f_1 and f_2 are independent functions. Standard mathematical treatment then shows that²⁵

$$f_1(r) \approx K_0(r/L_{eff}) \approx (r/L_{eff})^{-1/2} \exp\left[-\frac{r}{L_{eff}}\right], \quad (21)$$

where $K_0(u)$ is the modified Bessel function of the second kind, and that $f_2(z)$ has a sinusoidal dependence on z determined by the boundary conditions. One finally obtains

$$S = D \sqrt{\frac{1}{L_{eff}^2} - \frac{1}{L^2}} \tan \left[\sqrt{\frac{d^2}{L_{eff}^2} - \frac{d^2}{L^2}} \right]. \quad (22)$$

Because one generally has $D/L_{eff} \ll v_n$, the limit $S \approx v_n$ of very large S is obtained for $L_{eff} \approx 2d/\pi \ll L$ so that the argument of the tangent in Eq. (22) is $\approx \pi/2$. It is finally necessary to apply the model of the preceding section where the light excitation does not depend on lateral position, to the present experimental case where the light excitation is strongly focussed. For the calculation of $\Delta\phi$ at distance r , it is natural to replace in Eq. (13) N_0 by $N_0 f_1(r)$ in Eq. (13), where the value of $f_1(r)$, defined in Eq. (21), is $I_s(r)/I_s(0)$. One might expect that the strong radial dependence of the electron concentration causes a radial increase of S . However, it can be shown that this increase is averaged out. Indeed, the spatial dependence of $\Delta\phi$ induced by spatial variations $N_0 f_1(r)$ creates a drift current parallel to the surface in the depletion layer of magnitude $n_s \mu_n W_0 \delta\phi_b / \delta r = q W_0 n_s D / L_{eff}$, where $\mu_n = D k_B T / q$ is the electron mobility. This current produces a spatial averaging of n_s and therefore of S . The ratio of this current to the diffusion current in the film, $q d N_0 f_1(r) D / L_{eff}$, is equal to $(W_0/d) \exp[\phi_b / k_B T]$ and is very large. The slope of the experimental curves thus gives a well-defined value of S , related to a spatially averaged concentration $N_0 \langle f_1(r) \rangle$. This averaging does not perturb (i) the investigation of the relative change of surface recombination induced by passivation treatments, provided S is measured at constant values of photoelectron concentrations, (ii) the dependence of S on excitation power, and (iii) the value of the exponent η .

B. Samples

For the samples described in Fig. 2, the bulk charge and spin transport parameters were obtained using a GaInP passivated top surface that originally covered the sample and ensured a negligible surface recombination velocity. Investigations performed before the chemical removal of this surface GaInP layer yielded $L \approx 22 \mu\text{m}$ and $L_s \approx 1.2 \mu\text{m}$.²¹ Independent measurement of τ gives $D = 150 \text{ cm}^2/\text{s}$,²⁶ from which $T_1 \approx 0.96 \times 10^{-10} \text{ s}$ is estimated. This value is only a factor of two larger than the value found at 300 K for the same acceptor concentration in bulk GaAs of very distinct origin.²⁷

In order to illustrate the limiting cases underlined in Sec. II, five different samples were used, all characterized by the structure shown in Fig. 2 and by the same properties for bulk transport and recombination. The features of these samples and the results are summarized in Table I. Sample A has a naturally oxidized surface and the right panel of Fig. 2 shows the photo-luminescence spectrum and its degree of circular polarization for this case. One finds a degree of circular polarization of about 2%, thus revealing a photoelectron spin polarization of 4%. Sample B was obtained by

TABLE I. Summary of the measured values of the effective diffusion lengths for the samples shown in Fig. 3 at a power of $1 \mu\text{W}$. Estimated values of S , as obtained from Eq. (22), are also shown.

Sample	Details	L_{eff} (μm)	S (cm/s)
A	Naturally oxidized	2.2	3×10^6
B	Na_2S passivation	4.2	5.1×10^5
C	Encapsulation by 50 nm of GaInP	21.3	Negligible
D	HCl treatment	2	$>10^7$
E	Same as C after 3 years	8.9	4.8×10^4
E'	Same as C after 3.5 years	6.25	1.13×10^5

treating the oxidized surface for 1.5 min by a saturated sodium sulfide solution. This treatment is known to saturate Ga surface dangling bonds by sulfur atoms, and to reduce S by about one order of magnitude.²⁸ In order to illustrate the case of a negligibly small S (sample C), the results previously obtained for the GaInP encapsulated surface, reported in Ref. 21, are used. The case of infinite S is illustrated by a surface (sample D) obtained after extensive HCl pre-treatment, known to induce significant degradation of the surface.²⁹ Finally, sample E is identical to the GaInP-encapsulated sample C, but was investigated 3 years after growth in order to reveal ageing effects in the GaInP overlayer. A distinct piece of this sample, labelled E', was used for the investigation of the effect of light excitation power.

IV. RESULTS

A. Effect of passivation

The dependence of S on surface treatment is shown in Fig. 3 which presents the angular-averaged cross section of the sum image obtained for different surface terminations of the same GaAs films. In all cases, as seen from the dotted lines, L_{eff} was determined using Eq. (21) in a spatial range corresponding to identical photo-electron concentrations and S was found using Eq. (22). In the case of sample A (curve a, taken for a light excitation power of $1 \mu\text{W}$) $S = 3.0 \times 10^6$ cm/s which is close to 4.2×10^5 cm/s reported in Ref. 12 for an oxidized surface and a similar acceptor concentration. For sample B, curve b reveals a reduction in S of about one order of magnitude with respect to the oxidized surface as expected.²⁸ The extreme case of negligible S reveals the bulk properties of the GaAs and is shown in curve c for the GaInP-capped surface. This reproduces the results of Ref. 21. For sample D, we find $L_{\text{eff}} = 1.9 \mu\text{m} \approx 2d/\pi$ which, according to Eq. (22), corresponds to the case of infinite S . This sample illustrates the case of $S \approx v_n$. Curve e corresponds to $L_{\text{eff}} = 8.9 \mu\text{m}$ and reveals an increased $S = 4.8 \times 10^4$ cm/s with respect to sample C. This ageing effect has not, to the best of our knowledge, been previously reported for GaInP terminated surfaces, but could be due to the slow evolution of the existing GaInP disorder,³⁰ which is known to strongly affect the electronic properties.³¹

Shown in the inset of Fig. 3 are the cross sections of the difference images corresponding to curves a–e of the main figure. Immediately apparent is the fact that, unlike charge transport, spin transport depends only weakly on surface

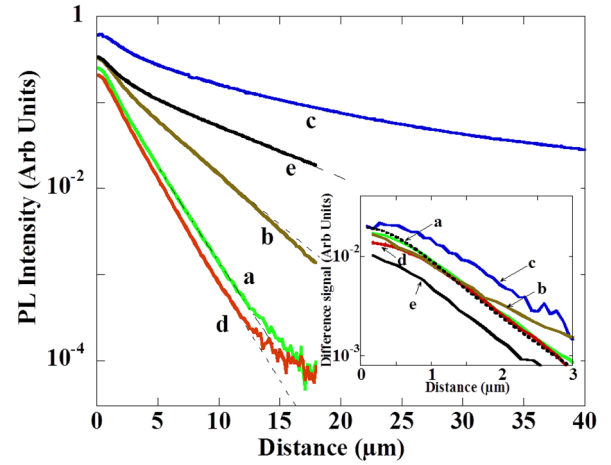


FIG. 3. Charge diffusion lengths and their fits by Bessel functions in order to determine L_{eff} and S for the naturally oxidized surface (curve a), and after treatment of the oxidized surface by Na_2S (curve b). The GaInP encapsulated surface (curve c, taken from Ref. 21 and shifted for clarity), corresponds to $L_{\text{eff}} = 21.3 \mu\text{m}$ and to a very small value of S . The surface treated by HCl and hydrazine sulfide (curve d) corresponds to $L_{\text{eff}} = 2 \mu\text{m}$ and to a very large value of S . Finally, the curve for the GaInP encapsulated surface about 3 years after growth (curve e) reveals slow degradation of the GaInP passivation. As shown in the inset, and unlike the latter sum profiles, the difference profiles are quite similar, because of the dominant effect of spin-lattice relaxation over surface recombination. The numerical calculation of the difference signal using the parameters of the oxidized surface corresponds very well, (dashed line) with no adjustable parameter, to the experimental curve a.

recombination and consequently the cross sections of the corresponding difference images are quite similar. This is expected since the effective spin lifetime is limited by spin-lattice relaxation (rather than by surface recombination) which only weakly depends on the surface treatment. For a quantitative interpretation, the analytical treatment summarized in Eqs. (18) and (19) is not valid since the distance to the excitation spot is comparable with the sample thickness. The dashed curve in the inset of Fig. 3 is a numerical solution of the spin diffusion equation for the case of the oxidized surface. This curve, obtained with no adjustable parameters, corresponds very well with the experimental curve a.

B. Effect of light excitation power

The effect of light excitation power P has been investigated between an extremely small value of about 1 nW and $5.7 \mu\text{W}$ for the samples A and E'. The inset of Fig. 4 shows the sum cross sections for the two samples for selected excitation powers and reveals an increase of L_{eff} with excitation power. This increase is from $1.9 \mu\text{m}$ to $2.3 \mu\text{m}$ for the oxidized surface, and from $3.5 \mu\text{m}$ to $7 \mu\text{m}$ for the encapsulated one. The corresponding values of S , calculated using Eq. (22), are shown in Fig. 5. For the oxidized surface at high power, one has $S = 2 \times 10^6$ cm/s, corresponding to the result of Fig. 3. A decrease in the power results in an increase in S by more than one order of magnitude so that, at low power, L_{eff} is close to $2d/\pi$ corresponding to the $S \approx v_n$ situation characterized by sample D. For the GaInP-encapsulated

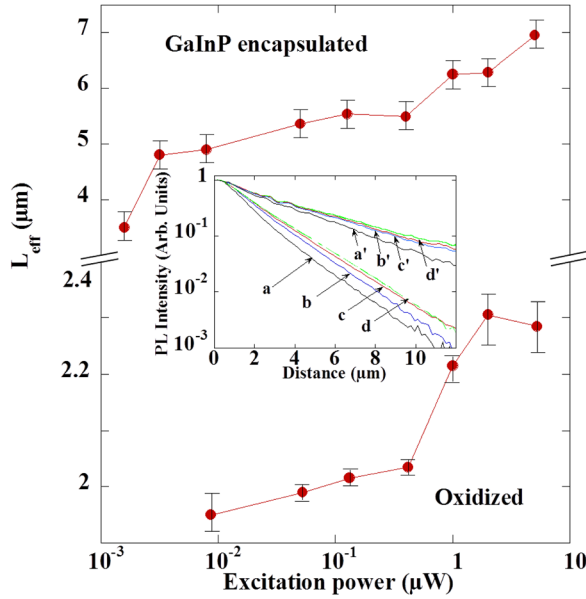


FIG. 4. Effect of excitation light power on the measured value of S . The inset shows the charge distribution profile for the oxidized sample for selected excitation powers: (a) 10^{-2} μW , (b) 0.45 μW , (c) 1.1 μW , and (d) 5.7 μW , and for the GaInP encapsulated surface for the same excitation powers (curves a' to d' , respectively). The main figure shows the dependences as a function of excitation power of the calculated values of L_{eff} .

surface on the other hand, S increases only by about a factor of 2 with an equivalent power decrease.

By monitoring the spatially averaged degree of circular polarization of the luminescence, defined as $\langle P \rangle = \langle I_d(r) \rangle / \langle I_s(r) \rangle$, higher excitation powers can be explored. Indeed, $\langle P \rangle$ is dominated by $n_+ - n_-$ and n at $r=0$, larger than their values at 10 μm by more than one order of magnitude. Shown in Fig. 6 are the dependences of $\langle P \rangle$ for the selected surfaces shown in Figs. 3 and 4 as a function of the values of S that are experimentally determined from the sum cross sections at $r = 10$ μm . Curve a shows the calculated dependence using a one dimensional resolution of the charge and spin diffusion equations for several values of S . For all data points, the surface recombination velocity at $r = 10$ μm is larger (by up to 1 order of magnitude) than the value deduced from $\langle P \rangle$. For the oxidized surface, $S = 3.0 \times 10^5$ cm/s corresponds well with an extrapolation of curve a of Fig. 5 to an excitation power of 1 mW . Conversely, for sample E', the experimental value of S almost coincides with its value calculated at $r=0$, in agreement with the weak power dependence of S for this sample.²⁶ As expected, the sulfide-passivated sample exhibits an intermediate behavior.

V. DISCUSSION

A. Comparison with the predictions of the model

The experimental results are in excellent agreement with the model of Sec. II. From a semi-quantitative approach, the dependence of S as a function of excitation power for the oxidized sample agrees with the power law predicted by Eq. (15) with an exponent of the order of 0.5. This gives $N_T(0)$ of the order of several 10^{12} cm^{-2}/eV which lies in the typical range of experimentally observed surface

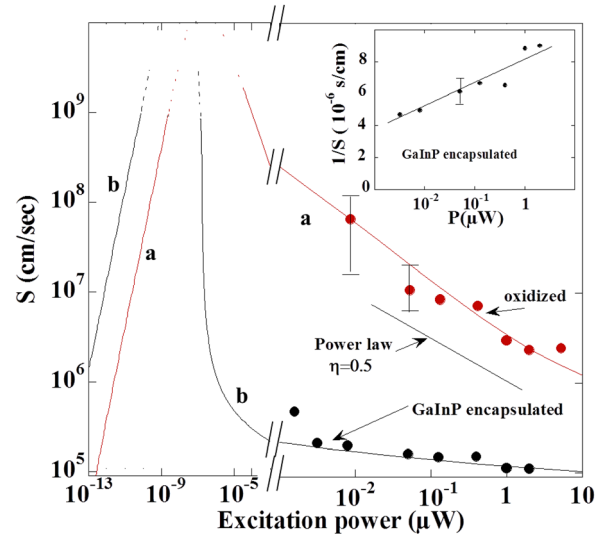


FIG. 5. The data points show the excitation power dependence of S , obtained from the results of Fig. 4 using Eq. (22). Note that the electronic concentration at the distance from the excitation spot at which S is measured corresponds to a homogeneous excitation power about two orders of magnitude smaller, for which we estimate that the density is 10^3 mW/cm^2 at a power of 1 μW . The solid lines show dependences calculated using Eqs. (6) and (12). For the oxidized surface, (curve a) the dependence is close to a power law, as predicted by Eq. (15) for $\eta \approx 0.5$, which gives a density of surface states $N_T \approx 10^{12}$ cm^{-2}/eV . For the GaInP-encapsulated surface (curve b), S is almost independent of P , because of the presence of a significant photoelectron concentration in the depletion layer. Also shown are extremely low (experimentally unreachable) powers, $P < 10^{-9}$ μW , at which S is predicted to increase with P . The inset shows that, for the GaInP encapsulated sample, as predicted by Eq. (16), S^{-1} increases linearly as a function of the logarithm of the power.

state concentrations.¹ The smaller power dependence of S for the encapsulated sample is viewed as the very high power regime illustrated by Eq. (16). As shown in the inset of Fig. 5, the inverse recombination velocity is approximately proportional to the logarithm of the excitation power. With respect to the oxidized sample, Eq. (15) would predict a

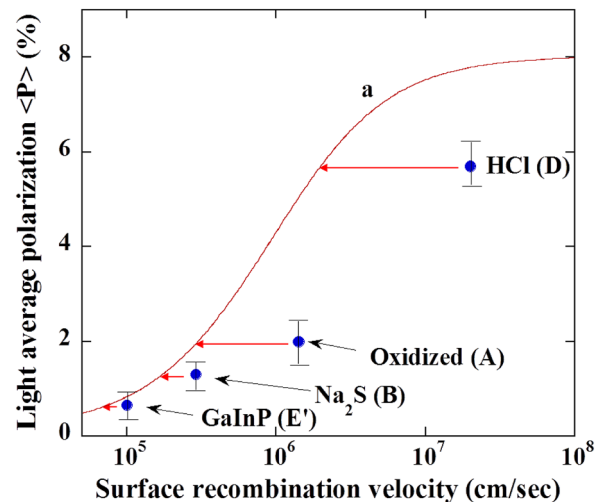


FIG. 6. Spatially integrated luminescence degree of circular polarization as a function of S measured for $P = 1$ μW and at $r \approx 10$ μm . Curve a is obtained using a numerical resolution of the charge and spin diffusion equations. The experimental results of Figs. 3 and 4 systematically correspond to S higher than the result of the calculation. This demonstrates the reduction of surface recombination velocity at the center, by an amount marked by arrows.

TABLE II. Parameter values used in the calculations of S as a function of power, for the encapsulated (E') and for the oxidized surface. Also shown are the equations where they are defined.

Definition	Equation	Encapsulated	Oxidized
$N_T(0)$ (cm ² /eV)	(5)	3×10^{10}	10^{12}
S_0 (cm/s)	(7)	1.3×10^{12}	4×10^{10}
ξ (at $1 \mu\text{W}$ and $r = 10 \mu\text{m}$)	(13)		10^6
N_0 (at $1 \mu\text{W cm}^{-3}$)	(B8)		4×10^{14}
v_d (cm/s)	(12)		10^4
γ_0	(17)		180

stronger power dependence because of the reduced value of $N_T(0)$. However, this effect is masked by the increase of the surface photo-electron concentration resulting from a reduction in S . As a result, K decreases because the second factor in Eq. (10) can be written $\exp[\gamma_0 v_d/S]$ and Eq. (16) must be applied.

Numerical resolution of Eqs. (6) and (12) enables a quantitative verification of the model of Sec. II. As shown in Table II, all parameter values, to be justified below, were unchanged for the two samples, with the exception of $N_T(0)$ and of S_0 which is related to $N_T(0)$ by Eqs. (5) and (7). Note that although S_0 may appear very large, the real value of S is much smaller. The quantities N_0 and v_d were calculated using Eqs. (B8) and (B11), respectively.

The obtained power dependences of S are shown by the solid lines of Fig. 5 and correspond very well with the experimental results for the two samples. It is also seen that the above choice of parameters gives acceptable values for three key quantities. For the surface barrier, expressed as $\phi_0 = k_B T \ln[N_A \gamma_0 \xi / N_0]$ we find 0.61 eV. The effective Richardson constant, obtained from $A^{**} = q T^{-2} v_d N_A \gamma_0$, is found equal to $3 \times 10^3 \text{ Am}^{-2} \text{ K}^{-2}$ which is a factor of 30 smaller than the value of the unreduced constant A for light holes. The difference can be attributed to the reduction of Schottky current due to the reduction in the probability of a majority carrier to reach the surface.³² Using Eq. (7), the value of S_0 is related to the hole capture cross section, expressed as

$$\sigma_p = (N_T(0) k_B T)^{-1} \frac{v_d^2}{S_0 v_p} \frac{N_A N_0 \gamma_0}{n_i^2 \xi}. \quad (23)$$

We estimate $\sigma_p \approx 10^{-6} \text{ cm}^2$. Although the accuracy is poor (the range of values of S_0 , γ_0 and ξ which allow us to interpret the data is of about 1 or 2 orders of magnitudes), this value is significantly larger than values of about 10^{-15} cm^2 measured by capacitance transient spectroscopy for bulk defects.³³ However, the present value may not seem unrealistic for at least three reasons: (i) it appears that trapping cross sections at defects of oxidized GaAs can be much larger than for bulk defects. Values as high as 10^{-9} cm^2 have been reported,³⁴ (ii) these values can further be increased by the probable presence of nanoclusters of elemental As,³⁵ in particular for the surface prepared by HCl decapping of GaInP,²⁹ and (iii) trapping of majority carriers in the flat band conditions used for capacitance spectroscopy overlooks tunnelling-assisted trapping over the top of the barrier. Such

an effect will obviously increase the effective concentration p_s of recombining majority carriers and induce a decrease of their energy by an amount δE . In Eq. (4), such an effect can be taken into account by an effective decrease of the bandgap and an increase of n_i^2 by $\exp[\delta E/k_B T]$, thus reducing the effective value of σ_p . Using Ref. 32, we calculate that values of δE of the order of 30% of the barrier are completely realistic, leading to a further decrease of σ_p by more than 3 orders of magnitude.

B. Dependence of S on surface state density and excitation power

In addition to being able to correctly interpret the experimental results on GaAs films, as shown in Appendix, the model summarized by Eqs. (14)–(16) is applicable to a wide class of semiconducting n- or p-type doped materials. As an example, the present model is in agreement with experimental results obtained on p-type silicon, for which a power law is also observed.²⁴ Using the results of the latter work at a resistivity of $10 \Omega \text{ cm}$, for which the precision is sufficient, we calculate using Eq. (9), $N_T(0) = 2 \times 10^{12} \text{ cm}^{-2} \text{ eV}^{-1}$, i.e., only a factor of 2 larger than the value obtained using a complete numerical calculation.¹⁴

These findings have three main implications for surface recombination studies which are at variance with the general picture of Ref. 5 in the particular case of doped semiconductors. First, the key role of light excitation power in the determination of S has been demonstrated even for extremely low powers. As a result, most values of S reported in the literature using photo-luminescence are likely to be underestimated because of the effect of Fermi level unpinning and cannot be considered as absolute determinations. As an example, the results of Fig. 5 at a power of $1 \mu\text{W}$ have been obtained with a value of $N_0 f_1(r)$ similar to the one used in Ref. 12. While the value of S for the oxidized surface is very close to that obtained by Ref. 12 for the same acceptor concentration, we conclude that a higher value of S , limited by the electron thermal velocity, would have been obtained for a reduced power level. If the power is reduced to extremely small values ($P < 10^{-15} \text{ W}$ for GaAs), S decreases and is smaller than v_n as shown in Fig. 5. While these small powers are experimentally unrealistic for GaAs, this regime has already been observed in silicon.²⁴ Thus, the quantity S_0 which is independent on photo-electron concentration can only be obtained from an analysis of the overall power dependence of S .

Second, we show here that the change of S induced by passivation is by far not proportional to the surface state concentration N_T , because of the passivation-induced changes of carrier concentrations at the surface [Eq. (4)]. At very low power, since S_0 is inversely proportional to $N_T(0)$, passivation should even result in an increase of S as shown in Fig. 5 and illustrated by Eq. (14). However, observation of this effect would require unattainably low excitation powers. For realistic powers, S further depends on $N_T(0)$ because of the dependence of $\Delta\phi$ on $N_T(0)$. Fig. 7 shows the calculated dependence of S as a function of N_T , under the combination of the two above effects, using the parameter values given in

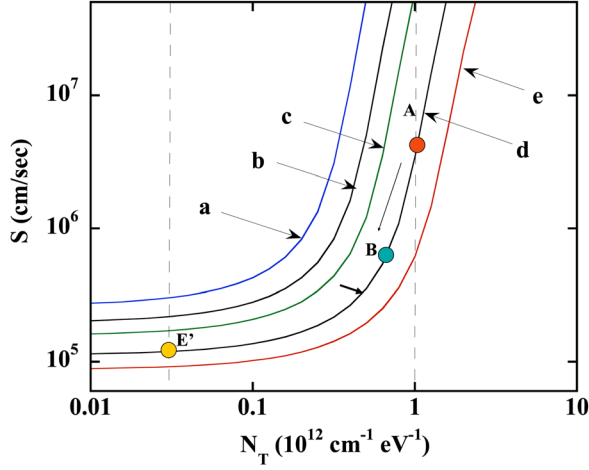


FIG. 7. Calculated dependence of S as a function of N_T for selected excitation powers. Curve d corresponds to an exciting power of $1 \mu\text{W}$ and to $N_0 \approx 4 \times 10^{14} \text{ cm}^{-3}$. Dots A, B, and E' correspond to the situation at a power of $1 \mu\text{W}$ of the oxidized surface, of the sulfide-passivated one, and of the GaInP-encapsulated one, respectively. The change from the regime described by Eq. (15) to the one described by Eq. (16) is shown by a short arrow in the figure, and occurs relatively abruptly. One sees that, because of its power dependence, S is far from proportional to N_T . As an example, the order of magnitude decrease of S induced by sulfide passivation (Fig. 4, curve b, also marked by a long arrow in the present figure) is caused by a decrease of N_T of only 25%. As seen from other curves, which correspond to values of P and N_0 multiplied by 10^{-4} (a), 10^{-3} (b), 10^{-2} (c), 10^2 (e), the passivation-induced change of S only weakly depends on power.

the preceding subsection. One sees that S does increase with $N_T(0)$. However, this dependence is far from proportional: (i) the decrease of S by one order of magnitude produced by the sulfide passivation of the oxidized surface in Fig. 3 implies a decrease of $N_T(0)$ by only 25%. (ii) For the GaInP-encapsulated sample E', corresponding to the regime described by Eq. (16), S is found to be almost independent on $N_T(0)$.

Third, the model presented here is able to qualitatively explain the dependence of S_0 on dopant concentration above 10^{16} cm^{-3} . For doping levels smaller than about 10^{16} cm^{-3} , the approximate proportionality between S and N_A or N_D depending on the semiconductor type,¹² has been interpreted as resulting solely from Eq. (4) which can be alternatively written for p-type material

$$S \propto N_T^*(0) \frac{\sigma_n v_n p_s}{n_0} = N_T^*(0) \frac{\sigma_n v_n N_A}{n_0} \exp\left[-\frac{\phi_b}{k_B T}\right]. \quad (24)$$

However, for the larger doping concentrations considered by the model, one observes a saturation of this dependence.¹² This result cannot be explained by Eq. (24) which would rather give a superlinear dependence because of the increased σ_n caused by the localization of minority carriers in the triangular potential well near the surface. The model presented here predicts that the N_A dependence of S , as defined by Eq. (15), is a combination of the decrease of $\xi^{-\eta}$ ($\eta \propto \sqrt{N_A}$) and of the increase of S_0 resulting from the increase of σ_p caused by tunnel-assisted trapping processes.

VI. CONCLUSION

We have shown in this work that the surface recombination velocity can be separated into a product of two factors dependent on excitation power via the photovoltage and the shift of the electron surface quasi Fermi level, respectively, and of a third, power-independent, factor which is inversely proportional to the surface state density. While direct verification of the latter highly counter-intuitive prediction is beyond the scope of the present work, it is strongly supported by the very good agreement with experimental results obtained in doped GaAs films as a function of light excitation power and passivation treatment.

While these results have been obtained for doped GaAs thin films, they are valid more generally for n- or p-type materials of doping level larger than 10^{16} cm^{-3} provided the surface barrier is not too small, and that surface recombination is dominated by the states which pin the Fermi level.

We outline three regimes as a function of excitation power and surface state density: (i) At extremely low power levels, such that the photovoltage is comparable or smaller than the thermal energy, S is predicted to increase with decreasing surface density and to increase with excitation power. Although these levels are too low to be reachable for GaAs, the increase as a function of power has been observed for silicon.¹⁴ (ii) For a larger excitation power, such that the photoelectron concentration in the depletion layer can still be neglected, S decreases with P as a power law for which the exponent depends on surface state density. The observed passivation-induced decrease of S can be caused by a very small change of surface center concentration. This case is illustrated by the naturally oxidized GaAs surface at realistic excitation powers. (iii) At high power or for a strongly reduced surface state density, the photoelectron concentration in the depletion layer can no longer be neglected. As a result, S^{-1} depends logarithmically on power and depends very weakly on surface state density. This situation is illustrated by the GaAs surface after encapsulation by GaInP.

ACKNOWLEDGMENTS

Two of us (V.L.B. and V.P.U.) are grateful to the French embassy in Moscow for sponsoring their research stay in France. F.C. is grateful to CONICYT Grant Becas Chile for supporting his work. The authors are grateful to G. Monier and C. Robert-Goumet for their participation in some experiments.

APPENDIX A: RANGE OF VALIDITY OF THE PRESENT MODEL

In this Appendix, we recall the various assumptions which allow us to obtain an analytical expression for S , and discuss their validity. Apart from general approximations such as equilibrium between bulk and surface, we have first neglected the photocurrent generated in the depletion layer. Thus, the present model is valid, for direct bandgap material, for a doping level larger than about 10^{16} cm^{-3} . Second, it has been assumed that recombination is limited by majority

carrier trapping. This implies that the surface barrier, taken here to 0.6 eV, should not be too small. Such approximation is justified from the relative magnitudes of the four terms of Eq. (4), given by for p-type material, by

$$\frac{n_{ts}}{n_s} = \frac{qN_c S_0}{A^{**} T^2} \exp\left[-\frac{E_G - \varphi_0}{k_B T}\right] \approx 10^{-9}, \quad (\text{A1})$$

$$\frac{\sigma_p v_p p_{ts}}{\sigma_n v_n n_s} = \frac{\sigma_p v_p q N_v S_0}{\sigma_n v_n A^{**} T^2} \exp\left[-\frac{\varphi_0 + 2\Delta\varphi}{k_B T}\right] \approx 7 \times 10^{-5} \frac{\sigma_p v_p}{\sigma_n v_n} \exp\left[-\frac{2\Delta\varphi}{k_B T}\right], \quad (\text{A2})$$

and

$$\frac{\sigma_p v_p p_s}{\sigma_n v_n n_s} = \frac{\sigma_p v_p q N_A S_0}{\sigma_n v_n A^{**} T^2} \exp\left[-\frac{\varphi_0 + 2\Delta\varphi}{k_B T}\right] \approx 8 \times 10^{-7} \frac{\sigma_p v_p}{\sigma_n v_n} \exp\left[-\frac{\Delta\varphi - \varphi_0 + \varphi_b}{k_B T}\right] \quad (\text{A3})$$

as a function of effective densities of states in the valence band N_v and conduction band N_c , respectively. The above numerical values are obtained by taking $\sigma_p/\sigma_n \approx 0.01$,¹⁴ and the values of $S_0/A^{**}T^2$ and of φ_0 obtained in Sec. V for the oxidized surface. As shown above, these ratios are indeed smaller than unity by several orders of magnitude. Conversely, for n-type material, recombination is also limited by trapping of majority carriers since $\sigma_p v_p p_s$ is found to be the dominant term. Both for n- and p-type materials, these ratios strongly increase upon reduction of φ_0 . For p-type material, the ratios of Eqs. (A2) and (A3) are larger than unity provided $\varphi_0 > 0.3$ eV below which the present model does not apply. Finally, it is also assumed here that $\Delta\varphi$ is smaller than the characteristic width of the energy-dependent density of surface states so that $N_T(\epsilon)$ is independent on energy. This excludes high injection conditions.

APPENDIX B: CALCULATION OF S

The equality of recombination current and photocurrent is first written, expressing $n_s p_s - n_{ts} p_{ts} = n_i^2 (\exp[qV_s/k_B T] - 1)$, where n_i is the intrinsic concentration

$$q n_0 S = J_{r0} \frac{N_T^*(\Delta\varphi)}{n_s} \left(\exp\left[\frac{qV_s}{k_B T}\right] - 1 \right), \quad (\text{B1})$$

where assuming equilibrium between the surface and the bulk, one has $n_s = n_0 \exp[\varphi_b/k_B T]$. Equations (2), (3), and (B1) then give

$$S = S_0 \exp[-\Delta\varphi/k_B T] (1 - \exp[-qV_s/k_B T]). \quad (\text{B2})$$

The charge neutrality equation is now used to express qV_s as a function of $\Delta\varphi$ so that S will be solely expressed as a function of $\Delta\varphi$. The negative light-induced surface charge must compensate the positive excess charge in the depletion layer so that one obtains

$$W_0 N_A \left[\sqrt{\frac{\varphi_b}{\varphi_0} + \frac{n_s k_B T}{N_A \varphi_0}} - 1 \right] = N_T(0) \Delta\varphi. \quad (\text{B3})$$

Here, W_0 is the equilibrium width of the depletion layer. The second term in the radical of Eq. (B3) is obtained by spatial integration of the photoelectron charge in the depletion layer.³⁶ The surface concentration is found from Eqs. (3) and (B2) to be $n_s = A^{**} T^2 \exp[\Delta\varphi/k_B T]/qS_0$. Using Eqs. (3) and (B3), we obtain

$$\exp\left[-\frac{qV_s}{k_B T}\right] = K \exp\left[-(1 + \eta^{-1}) \frac{\Delta\varphi}{k_B T}\right], \quad (\text{B4})$$

where K and η are given by Eqs. (10) and (9), respectively. Using Eqs. (B2) and (B4), one obtains Eq. (6). Again using $J_p = J_r$ and Eq. (6) one also finds

$$K \exp\left[-(1 + \eta^{-1}) \frac{\Delta\varphi}{k_B T}\right] = (q n_0 S_0 / J_0)^{-1}. \quad (\text{B5})$$

Equations (6) and (B5) are used to calculate $\Delta\varphi$ and therefore S as a function of the excess concentration n_0 . This type of analytical treatment is analogous to the numerical approach used elsewhere.¹⁴ In itself however, it is insufficient since n_0 also depends on S .

Finally, in order to obtain an explicit expression for S on excitation power, n_0 must be calculated by solving (in a unipolar regime at low excitation power²⁶) the diffusion equation for the photo-electron concentration n in the bulk of the semiconductor

$$g\tau\phi(r)\alpha\exp[-\alpha z] - n + L^2\Delta n = 0, \quad (\text{B6})$$

where r is the distance to the excitation spot and z is the depth coordinate. Here, $L = \sqrt{D\tau}$, related to the diffusion constant D and to the bulk minority carrier lifetime τ , is the diffusion length, Δ is the Laplacian operator, α is the light absorption coefficient, and g is the rate of electron-hole pair creation. The function $\phi(r)$ describes the light profile and is assumed in this model to be constant. Using the boundary conditions $D\partial n/\partial z = Sn$ for the front surface, and $D\partial n/\partial z = -S'n$ at the back surface of the sample of thickness d , it is found that

$$n_0 = \beta N_0 = \frac{v_d}{v_d + S} N_0, \quad (\text{B7})$$

where v_d is the diffusion velocity which gives a measure of bulk recombination and N_0 is a reduced photoelectron concentration. The general expressions for N_0 and v_d , which are strongly simplified in the present case where $S' = 0$, are

$$N_0 = \frac{g\alpha\tau}{(\alpha L)^2 - 1} \frac{\mathcal{N}}{\mathcal{D}} \quad (\text{B8})$$

with

$$\mathcal{N} = \alpha L \left(\cosh \frac{d}{L} - e^{-\alpha d} \right) - \sinh \frac{d}{L} + \frac{S'L}{D} \left[e^{-\alpha d} - \cosh \frac{d}{L} + \alpha L \sinh \frac{d}{L} \right], \quad (\text{B9})$$

$$\mathcal{D} = \frac{S'L}{D} \cosh \frac{d}{L} + \sinh \frac{d}{L}, \quad (\text{B10})$$

and

$$v_d = \frac{D}{L} \left[\frac{\sinh \frac{d}{L} + S'L/D \cosh \frac{d}{L}}{\cosh \frac{d}{L} + S'L/D \sinh \frac{d}{L}} \right]. \quad (\text{B11})$$

Because v_d depends on d , it is very large for semi-infinite samples and n_0 is independent of S . This is not the case for thin films. Finally, Eq. (12) is obtained using Eqs. (6), (B5), and (B7).

- ¹H. Hasegawa, M. Akazawa, A. Domanowska, and B. Adamowicz, *Appl. Surf. Sci.* **256**, 5698 (2010).
- ²W. E. Spicer, T. Kendelewicz, N. Neuman, R. Cao, C. McCants, K. Miyano, I. Lindau, Z. Liliental-Weber, and E. R. Weber, *Appl. Surf. Sci.* **33–34**, 1009 (1988).
- ³H. Hasegawa and H. Ohno, *J. Vac. Sci. Technol. B* **4**, 1130 (1986).
- ⁴C. Chang, C. Chi, M. Yao, N. Huang, C. Chen, J. Theiss, A. Bushmaker, S. LaLumondiere, T. Yeh, M. Povinelli et al., *Nano Lett.* **12**, 4484 (2012).
- ⁵D. Aspnes, *Surf. Sci.* **132**, 406 (1983).
- ⁶M. Polignano, N. Bellaiofiore, D. Caputo, A. Caricato, A. Modelli, and R. Zonca, *J. Electrochem. Soc.* **146**, 4640 (1999).
- ⁷Y. Ogita, *J. Appl. Phys.* **79**, 6954 (1996).
- ⁸G. Storr and D. Haneman, *J. Appl. Phys.* **58**, 1677 (1985).
- ⁹L. Jastrzebski, H. Gatos, and J. Lagowski, *J. Appl. Phys.* **48**, 1730 (1977).
- ¹⁰D. Wittry and D. Kyser, in *Proceedings of the International Conference of the Physics of Semiconductors*, Kyoto, 1966 [J. Phys. Soc. Jpn. Suppl. 21 (1966)].
- ¹¹K. Mettler, *Appl. Phys. A: Mater. Sci. Process.* **12**, 75 (1977).
- ¹²H. Ito and T. Ishibashi, *Jpn. J. Appl. Phys., Part 1* **33**, 88 (1994).
- ¹³R. Ahrenkiel and S. Johnston, *Sol. Energy Mater. Sol. Cells* **93**, 645 (2009).
- ¹⁴A. Aberle, S. Glunz, and W. Warta, *J. Appl. Phys.* **71**, 4422 (1992).
- ¹⁵J. M. Moison, M. Van Rompay, and M. Bensoussan, *Appl. Phys. Lett.* **48**, 1362 (1986).
- ¹⁶R. Aleksiejunas, M. Sudzius, T. Malinauskas, J. Vaitkus, K. Jarasiunas, and S. Sakai, *Appl. Phys. Lett.* **83**, 1157 (2003).
- ¹⁷R. Cuscó, J. Ibáñez, E. Alarcón-Lladó, L. Artús, T. Yamaguchi, and Y. Nanishi, *Phys. Rev. B* **80**, 155204 (2009).
- ¹⁸H. Wang, K. Wong, B. Foreman, Z. Yang, and G. Wong, *J. Appl. Phys.* **83**, 4773 (1998).
- ¹⁹Y. Cui, M. Groza, D. Hillman, A. Burger, and R. James, *J. Appl. Phys.* **92**, 2556 (2002).
- ²⁰T. Saitoh and H. Hasegawa, *Appl. Surf. Sci.* **56**, 94 (1992).
- ²¹I. Favorskiy, D. Vu, E. Peytavit, S. Arscott, D. Paget, and A. Rowe, *Rev. Sci. Instrum.* **81**, 103902 (2010).
- ²²D. Vu, S. Arscott, E. Peytavit, R. Ramdani, E. Gil, Y. André, S. Bansropun, B. Gérard, A. Rowe, and D. Paget, *Phys. Rev. B* **82**, 115331 (2010).
- ²³E. Yablonovitch, R. M. Swanson, W. D. Eades, and B. R. Weiberger, *Appl. Phys. Lett.* **48**, 245 (1986).
- ²⁴A. Stephens, A. Aberle, and M. Green, *J. Appl. Phys.* **76**, 363 (1994).
- ²⁵S. Visvanathan and J. Battey, *J. Appl. Phys.* **25**, 99 (1954).
- ²⁶D. Paget, F. Cadiz, A. Rowe, F. Moreau, S. Arscott, and E. Peytavit, *J. Appl. Phys.* **111**, 123720 (2012).
- ²⁷K. Zerrouati, F. Fabre, G. Bacquet, J. Bandet, J. Frandon, G. Lampel, and D. Paget, *Phys. Rev. B* **37**, 1334 (1988).
- ²⁸D. Paget, A. Gusev, and V. Berkovits, *Phys. Rev. B* **53**, 4615 (1996).
- ²⁹M. Kang, S. Sa, H. Park, K. Suh, and K. Oh, *Thin Solid Films* **308**, 634 (1997).
- ³⁰J. Leong, J. McMurray, C. Williams, and G. Stringfellow, *J. Vac. Sci. Technol. B* **14**, 3113 (1996).
- ³¹A. Sasaki, K. Tsuchida, Y. Narukawa, Y. Kawakami, S. Fujita, Y. Hsu, and G. Stringfellow, *J. Appl. Phys.* **89**, 343 (2001).
- ³²E. Rhoderick, *Metal Semiconductor Contacts* (IET, 1982).
- ³³C. Henry and D. Lang, *Phys. Rev. B* **15**, 989 (1977).
- ³⁴P. Deenapanray, H. Tan, and C. Jagadish, *Appl. Phys. A: Mater. Sci. Process.* **76**, 961 (2003).
- ³⁵P. Brunkov, V. Chaldyshev, A. Chernigovskii, A. Suvorova, N. Bert, S. Konnikov, V. Preobrazhenskii, M. Puyato, and B. Semyagin, *Semiconductors* **34**, 1068 (2000).
- ³⁶L. Kronik and Y. Shapira, *Surf. Sci. Rep.* **37**, 1 (1999).